Asian Journal of Chemistry; Vol. 26, No. 15 (2014), 4767-4770

ASIAN JOURNAL OF CHEMISTRY

http://dx.doi.org/10.14233/ajchem.2014.16205

Synthesis of Metal Ion Doped Sr_2CeO_4 by Hydrothermal Method and Its Luminescent Properties

YONG-QING ZHAI*, ZHI-CHUN HU, JIAN MA, XUAN LI and JIN-HANG LI

*College of Chemistry and Environmental Science, Hebei University, Baoding 071002, P.R. China

*Corresponding author: Fax: +86 312 5079525; E-mail: zhaiyongqinghbu@163.com

Received: 19 August 2013; *Accepted*: 14 November 2013; *Published online*: 16 July 2014; AJC-15568

Blue-white emitting phosphor Sr_2CeO_4 and a series of Sr_2CeO_4:M(M = Mg, Ca, Zn, Al) were synthesized by hydrothermal method using $(NH_4)_2CO_3$ as the precipitation agent. Phase structure and luminescence properties of the as-synthesized phosphors were investigated by X-ray diffraction and fluorescence spectrophotometry respectively. Results show that Sr_2CeO_4:M (M = Mg, Ca, Zn, Al) phosphors have the same orthorhombic crystal structure as that of Sr_2CeO_4. Doping with metal ions has little effect on shape and position of peaks in emission spectrum of Sr_2CeO_4, which is located in the range of 400-600 nm with main peak at 466 nm and ascribed to the $f \rightarrow t_{1g}$ transition of Ce^{4+} ions. Among these metal ions, doping with Zn^{2+} or Mg^{2+} can effectively enhance the photoluminescence of Sr_2CeO_4 phosphor, the appropriate doping concentration of Zn^{2+} and Mg^{2+} is 5 and 4 %, respectively. Moreover, a red-shift is found in the excitation spectrum of Sr_2CeO_4 phosphor after doping with Zn^{2+} or Mg^{2+}.

Keywords: Sr_2CeO_4, Metal ion-doping, Hydrothermal synthesis, Photoluminescence.

INTRODUCTION

It is well known that oxide-based phosphors have been widely utilized in the fields of optoelectronics and display devices due to their high thermal stability and chemical stability[1,2]. Danielson *et al.*[3] have successfully synthesized a unusual rare-earth oxide phosphors Sr_2CeO_4 by combinatorial technique, emitting a blue-white fluorescence by the excitation through the ultraviolet ray, cathode ray or X-ray. Further research suggests that the emission of Sr_2CeO_4 is originated from Ce^{4+} to O^{2-} charge transfer (CT) transition. The broad excitation spectrum in the 200-400 nm range indicated the feasibility of Sr_2CeO_4 phosphor utilized in UV-LED. Moreover, owning to its broad emission band, Sr_2CeO_4 can also be used as the matrix materials. Until now, the rare earth-doped Sr_2CeO_4 (Sr_2CeO_4: Ln = Eu, Dy, Sm, Ho, Er, Tm) has been widely investigated as a kind of fluorescent materials. Rao *et al.*[4] synthesized Sr_2CeO_4: Eu^{3+}, La^{3+} phosphor by solid state reaction method, which could be used in white light emitting display devices. Shi *et al.*[5] found that by turning of the concentration of Eu^{3+}, Sr_2CeO_4: Eu^{3+} could provide a foundation for potential application in single-color or two-color fluorescence thermometry techniques. But, Pieterson *et al.*[6] pointed that Sr_2CeO_4 was difficult to be used as commercial phosphor, because the quantum efficiency (QE) of Sr_2CeO_4 was less than 50 % at room temperature, which was too low to compete with the presently used materials with a quantum efficiency between 80~90 %. Therefore, how to improve the luminescence of Sr_2CeO_4 has become much more attractive and necessary.

Many researches showed that impurity ions could produce a change of symmetry and vibration modes around the luminescence center to result in the enhancement of the luminescence intensity[7-9]. Therefore, in this paper, Sr_2CeO_4 and impurity ions doped Sr_2CeO_4:M (M = Mg, Ca, Zn, Al) phosphors were synthesized by hydrothermal method using $(NH_4)_2CO_3$ as the precipitation agent. Moreover, phase structure and luminescence properties of the phosphors were investigated by X-ray diffraction and fluorescence spectrophotometry respectively.

EXPERIMENTAL

$Sr(NO_3)_2$, $Ce(NO_3)_3{\cdot}6H_2O$, $Mg(NO_3)_2{\cdot}6H_2O$, $Ca(NO_3)_2{\cdot}4H_2O$, $Zn(NO_3)_2{\cdot}6H_2O$, $Al(NO_3)_3{\cdot}9H_2O$, $(NH_4)_2CO_3$. were used as starting materials. They were all analytical reagents (A.R.).

Detailed procedure was as follows: The appropriate stoichiometric proportion of $Sr(NO_3)_2$, $Ce(NO_3)_3{\cdot}6H_2O$ and metal nitrate were dissolved in deionized water and fully stirred. Then$(NH_4)_2CO_3$ was dropped slowly into the above solution to adjust the pH value to 9. After 0.5 h of stirring, the mixture was transferred into a teflon-lined stainless steel autoclave with a capacity of 75 %. Hydrothermal reaction was carried out at 180 °C for 6 h and then cooled to room temperature. The obtained suspension was filtered and filter cake washed with distilled water and a little amount of alcohol. The obtained precursor was put into an oven and dried at 90 °C for 4 h. Finally, the precursor was calcined in a muffle furnace at 1100 °C for 2 h in air.

Phases and crystallization structure of the samples were analyzed and characterized by a Y-2000 X-ray diffractometer using CuK$_\alpha$ radiation (30 kV × 20 mA, scanning speed 0.06 °/s and λ = 1.54178 Å). The excitation and emission spectra of the samples were recorded as pellets on an F-380 fluorescence spectrometer. All samples were performed at room temperature.

RESULTS AND DISCUSSION

X-ray diffraction analysis: Fig. 1 shows the X-ray diffraction patterns of un-doped Sr_2CeO_4 and a series of $Sr_{1.9}M_{0.1}CeO_4$ (M = Mg, Ca, Zn, Al) powders obtained by calcining the hydrothermal precursor at 1100 °C for 2 h. From Fig. 1, it can be seen that nearly all of the peaks of un-doped Sr_2CeO_4 and $Sr_{1.9}M_{0.1}CeO_4$ (M = Mg, Ca, Zn) can be indexed to the Sr_2CeO_4, which agrees well with the JCPDS card (No. 50-0015). According to that, series of samples are orthorhombic phase Sr_2CeO_4 with space group Pbam. In these patterns, the peaks of compounds of Mg, Ca or Zn cannot be found, which indicates that Mg^{2+}, Ca^{2+} and Zn^{2+} ions have entered into the host lattice and have little effect on the crystal structure of the host Sr_2CeO_4.

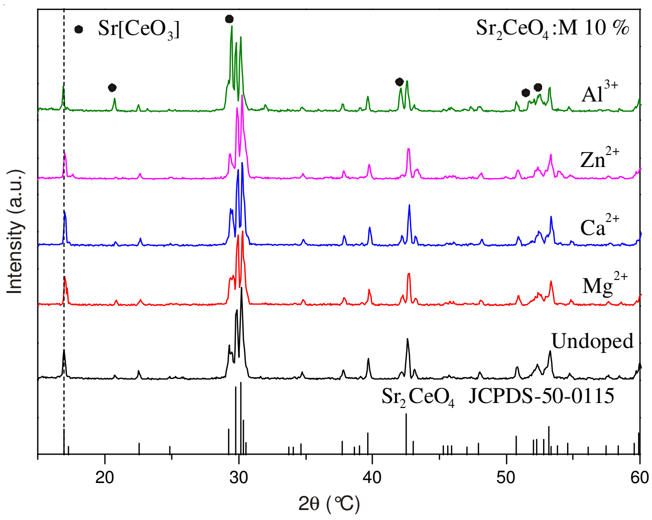

Fig. 1. XRD patterns of un-doped Sr_2CeO_4 and $Sr_{1.9}M_{0.1}CeO_4$ (M = Mg, Ca, Zn, Al) powders

As shown in Fig. 1, the X-ray diffraction peaks of un-doped Sr_2CeO_4 are good agreement with the standard values in JCPDS card (No. 50-0015). However, with the doping of Mg^{2+}, Ca^{2+} or Zn^{2+}, the position of diffraction peaks of Sr_2CeO_4 is deviated to the right, it is because that the smaller radius Mg^{2+} (R = 0.065 nm), Ca^{2+} (R = 0.099 nm) or Zn^{2+} (R = 0.074 nm) ions substitute larger radius Sr^{2+} (R = 0.113) ions in the crystals lattice, which lead to the decrease of lattice parameters and crystal plane spacing. According to the bragg equation, $2d\sin\theta = \lambda$, where d is the crystal plane spacing, θ the diffraction peak angle and λ the radiation wavelength (1.54178 Å for CuK$_\alpha$), thus the θ increases as the d reduces. Therefore, compared with un-doped Sr_2CeO_4, the diffraction peaks of $Sr_{1.9}M_{0.1}CeO_4$ (M = Mg, Ca, Zn) moves toward large angle (toward right). However, the doping of Al^{3+} ions has little effect on the position of diffraction peaks and the phase of $Sr[CeO_3]$ begin to appear. The possible reason is as follows: the radius of Al^{3+} (R = 0.05 nm) is small enough to occupy any crystal lattice site, it could be located at the sites of Sr^{2+} and Ce^{4+}, moreover could reside in interstitial sites between or among the host ions. Despite the fact that the radius of Al^{3+} is smaller than that of Sr^{2+} or Ce^{4+}, the size is larger than interstitial site, which results in the cell volume of Sr_2CeO_4 becoming larger and effecting the reaction process[10-11].

Emission spectra of Sr_2CeO_4 and $Sr_{1.9}M_{0.1}CeO_4$ (M = Mg, Ca, Zn or Al): Under ultraviolet (UV) radiation at 292 nm, all the samples show bright blue-white emitting. Fig. 2 shows the emission spectra of the samples Sr_2CeO_4 and $Sr_{1.9}M_{0.1}CeO_4$ (M = Mg, Ca, Zn or Al) obtained by calcining the hydrothermal precursor at 1100 °C for 2 h. As show in Fig. 2(c), the emission spectra of Sr_2CeO_4 show broad band in the region 400-600 nm with a peak around 466 nm. The emission band is assigned to the $f \rightarrow t_{1g}$ transitions of Ce^{4+} ions, which determined by the special one-dimensional chain structure of Sr_2CeO_4. In the Sr_2CeO_4 structure, there are two different band length Ce-O in CeO_6 octahedra, that is Ce-O and Ce-O-Ce and the Ce-O distance is about 0.1 Å shorter than the Ce-O-Ce, which is a critical factor to observation of charge transfer luminescence. The shape and position of the emission spectra of the metal ion doped Sr_2CeO_4 powders are similar to that of the pure Sr_2CeO_4 powder, corresponding to the charge-transfer transition from Ce^{4+} to O^{2-} in the matrix and the result shows that the metal ions doping does not change the luminescence centre and the luminescence mechanism of the phosphors. It is found that the doping with Al^{3+} or Ca^{2+} can reduce the fluorescence intensity of Sr_2CeO_4 phosphors, however, the luminous intensity of the Zn^{2+} or Mg^{2+} doped Sr_2CeO_4 powders is found to be enhanced effectively.

For Ca^{2+}, Mg^{2+}, Zn^{2+}, Al^{3+} and Sr^{2+} ions, the ionic radii are 0.099, 0.065, 0.074, 0.05 and 0.113 nm, respectively. Doping with Al^{3+} reduce the fluorescence intensity of the Sr_2CeO_4, there are two reasons about it: one is that Al^{3+} ions substitute partially Sr^{2+} ions when they enter into the crystal sites, it is a unequivalent substitution, which will damage the charge balance of the host Sr_2CeO_4; the other is that Al^{3+} ions can easily reside in interstitial sites in the Sr_2CeO_4 lattice because of its small size, therefore, the symmetry would be destroyed by the interstitial Al^{3+} and the charge-transfer transition from Ce^{4+} to O^{2-} become difficulty[11]. Pieterson *et al.*[5] have studied the luminous intensity of Ca-doped Sr_2CeO_4 and observed a red shift of the emission, which was attributed to the expansion of the metal-to-ligand bonds in the excited state as a result of the presence of a smaller Ca^{2+} ion on a larger Sr^{2+} site and the emission spectra relative intensity will decrease. The same phenomenon is also observed in our present study. Doping Ca^{2+} ions in Sr_2CeO_4 lead to the red-shift of about 4 nm in the emission spectrum and a great decrease of the fluorescence intensity. The size of Mg^{2+} and Zn^{2+} is smaller than Sr^{2+}, but the red-shift in the emission spectra of Mg^{2+} or Zn^{2+}-doped Sr_2CeO_4 powders is not clearly observed and the fluorescence intensity is improved, which can be associated with the larger pauling electonegativity of Mg^{2+} and Zn^{2+} .

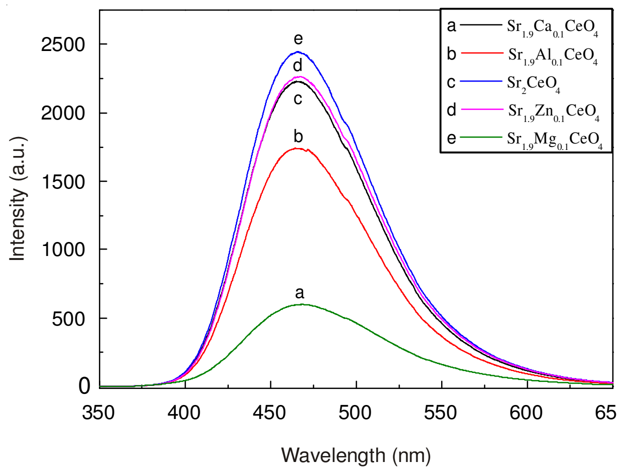

Fig. 2. Emission spectra of un-doped Sr_2CeO_4 and $Sr_{1.9}M_{0.1}CeO_4$ (M = Mg, Ca, Zn, Al) powders

Effect of Zn^{2+} concentration on luminescence properties of Sr_2CeO_4: In order to investigate the effect of Zn^{2+} concentration (x) on luminescent properties of the samples, a series of samples $Sr_{2-x}Zn_xCeO_4$ (X = 0.05, 0.1, 0.15) with different Zn^{2+} concentration were synthesized and their excitation spectra are shown in Fig. 3. All the excitation spectra of $Sr_{2-x}Zn_xCeO_4$ phosphors show a broad band around 286 nm with a shoulder at 336 nm, which is attributed to the charge transfer band of Ce^{4+}-O^{2-}. Compared with pure Sr_2CeO_4 powders, a clear red shift occurs in the excitation spectra of Zn-doped Sr_2CeO_4 and the main peak is red-shift from 286 nm to 292 nm. We considered that Zn^{2+} substitute partially Sr^{2+} ions in the crystalline lattice, but Zn^{2+} can attract the electrons of O^{2-} more strongly than the Sr^{2+} because of the larger electronegativity ($\chi(Zn^{2+}) = 1.65$ and $\chi(Sr^{2+}) = 0.95$), which result in decreasing the electron density around O^{2-} ion. Thus, the electron transition from the Ce^{4+} to O^{2-} is liable to carry out when excited and the charge-transfer state band is shifted toward lower energy.

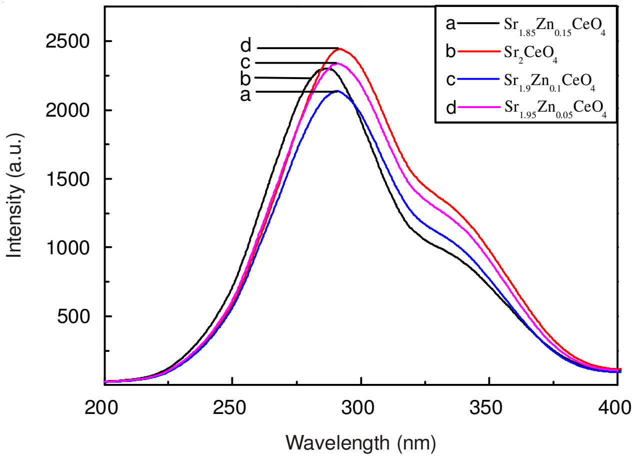

Fig. 3. Excitation spectra of $Sr_{2-x}Zn_xCeO_4$ powders

Fig. 4 shows that the emission spectra of all the Zn-doped Sr_2CeO_4 phosphors excited by the maximum excitation wavelength. It can be see that the Zn^{2+} concentration has little effect on the shape and position of emission peaks, which is located in the range of 400-600 nm with the main peak at 466 nm, but has great effect on the intensity. It is found that the emission intensity of $Sr_{2-x}Zn_xCeO_4$ powders increases at first, then decreases with the increase of Zn content. The emission intensity is up to the highest when x = 0.05. Xue *et al.*[12] have studied the luminescence property of Sr_2CeO_4 doped with Zn^{2+}. They considered that the possibility of the emission from the O^{2-} to Ce^{4+} transition is expected to be enhanced in Zn-doped Sr_2CeO_4 as a result of the larger electronegativity and the smaller radius of Zn^{2+} ions; excessive Zn^{2+} addition increase the mutual interatomic interaction, which results in the decreasing of the emission from the O^{2-} to Ce^{4+} transition.

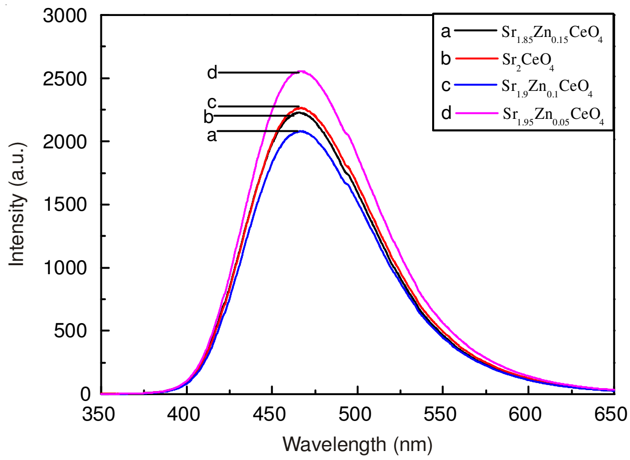

Fig. 4. Emission spectra of $Sr_{2-x}Zn_xCeO_4$ powders

Effect of Mg^{2+} concentration on luminescence properties of Sr_2CeO_4: Fig. 5 shows the excitation spectra (monitored at 466 nm) of the samples $Sr_{2-x}Mg_xCeO_4$ (x = 0.02, 0.04, 0.1, 0.15). It can be seen that the concentration of Mg^{2+} has little effect on the shape of the excitation spectra, showing a wide band with double peaks in the range of 200-400 nm. Introduction of Mg^{2+} ions leads to a red-shift of about 2 nm in the excitation spectra, which is shorter than that of Zn-doped Sr_2CeO_4. The reason is that the electronegativity of Mg^{2+} ($\chi = 1.31$) is larger than that of Sr^{2+}, but smaller than that of Zn^{2+}, which results in the ability of attracting the electrons of O^{2-} is higher Sr^{2+}, but lower Zn^{2+}. Therefore, the red shift of CTS band becomes shorter.

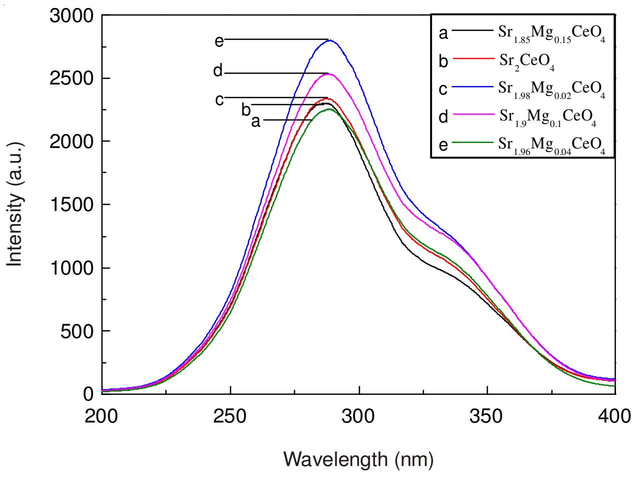

Fig. 5. Excitation spectra of $Sr_{2-x}Mg_xCeO_4$ powders

Fig. 6 shows that the emission spectra of all the Mg-doped Sr_2CeO_4 phosphors excited by the maximum excitation wavelength. It is found that the Mg^{2+} concentration has little effect on the shape and position of emission peaks, but has great effect on the intensity. When Mg^{2+} doping concentration x = 0.04, the emission intensity reaches the maximum value. The emission intensity begins to decrease when x > 0.04. Therefore, it can be known that the appropriate doping amount of Mg^{2+} (x = 0.04) can improve luminescent intensity of the sample significantly.

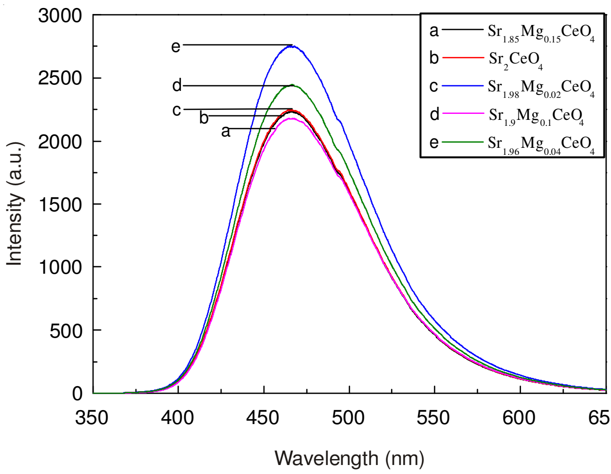

Fig. 6. Emission spectra of $Sr_{2-x}Mg_xCeO_4$ powders

Conclusion

Blue-white emitting phosphor undoped and metal ions doped Sr_2CeO_4 phosphors were synthesized by hydrothermal method using $(NH_4)_2CO_3$ as the precipitation agent. It is found that Mg^{2+}, Ca^{2+} or Zn^{2+} doped phosphors can keep the crystal structure of the host Sr_2CeO_4 and the position of diffraction peaks of Sr_2CeO_4 is deviated to the right. While Al^{3+} doped phosphors have impurity phase of $Sr[CeO_3]$ and the position of diffraction peaks is not deviated to the right. Moreover, the dependences of the photoluminescence on doping species and doping concentration have been investigated. It is found that Zn^{2+} and Mg^{2+} doping with a appropriate concentration x = 0.05 and 0.04, respectively can effectively enhance the photoluminescence of Sr_2CeO_4 phosphors. This investigation provides a new way to enhance the luminescent properties of the Sr_2CeO_4 phosphor by using metal ions impurity doping. Thus, the results may be very useful for the application of the Sr_2CeO_4 phosphor in future display devices.

ACKNOWLEDGEMENTS

This study was supported by National Natural Science Foundation of China (No. 50672020).

REFERENCES

1. G.F. Wang, Q.Y. Mu, T. Chen and Y.D. Wang, *J. Alloys Comp.*, **493**, 202 (2010).
2. J.L. Huang, L.Y. Zhou, Z.L. Wang, Y.W. Lan, Z.F. Tong, F.Z. Gong, J.H. Sun and L.P. Li, *J. Alloys Comp.*, **487**, L5 (2009).
3. E. Danielson, M. Devenney, D.M. Giaquinta, J.H. Golden, R.C. Haushalter, E.W. McFarland, D.M. Poojary, C.M. Reaves, W.H. Weinberg and X.D. Wu, *Science*, **279**, 837 (1998).
4. C.A. Rao, P.R.V. Nannapaneni and K.V.R. Murthy, *Adv. Mater. Lett.*, **4**, 207 (2013).
5. L.L. Shi, H. J. Zhang, C. Y. Li and Q. Su, *RSC Adv.*, **1**, 298 (2011).
6. L. van Pieterson, S. Soverna and A. Meijerink, *J. Electrochem. Soc.*, **147**, 4688 (2000).
7. M.K. Chong, K. Pita and C.H. Kam, *Appl. Phys. A*, *Mater. Sci. Process.*, **79**, 433 (2004).
8. K. Park, M.N. Heo, Y. Kim and J.Y. Kim, *J. Nano Res.*, **18**, 257 (2012).
9. W. Yue, J.L. Yan, J.Y. Wu and L.Y. Zhang, *J. Semicond.*, **33**, 073003 (2012).
10. L.L. Shi, C.Y. Li and Q. Su, *J. Alloys Comp.*, **509**, 4209 (2011).
11. T.S. Atabaev, H.H. Thi Vu, Z. Piao, Y.-H. Hwang and H.-K. Kim, *J. Alloys Comp.*, **541**, 263 (2012).
12. S.W. Xue, E.G. Wang and J. Zhang, *Chinese Phys. B*, **20**, 078105 (2011).